

RELAXATION TIME FOR A DIMER COVERING WITH HEIGHT REPRESENTATION

Christopher L. Henley

Dept. of Physics, Cornell University, Ithaca NY 14853-2501

This paper considers the Monte Carlo dynamics of random dimer coverings of the square lattice, which can be mapped to a rough interface model. Two kinds of slow modes are identified, associated respectively with long-wavelength fluctuations of the interface height, and with slow drift (in time) of the system-wide mean height. Within a continuum theory, the longest relaxation time for either kind of mode scales as the system size N . For the real, discrete model, an exact *lower* bound of $O(N)$ is placed on the relaxation time, using variational eigenfunctions corresponding to the two kinds of continuum modes.

I. INTRODUCTION

One of the simplest lattice statistical models is the dimer covering of the square lattice [1,2]. The dimers are placed on the bonds and every site must be touched by exactly one dimer. (This is equivalent, of course, to the packings of “dominoes” of size 2×1 [3]; furthermore the ground states of the fully frustrated Ising model on the square lattice map 2-to-1 to the dimer coverings [4].) In this paper, I only consider the case where each packing has equal weight. The system is taken to be a square of $L \times L$ sites.

The statics can be described by mappings to free fermions and exact solutions exist using Pfaffians [1,2] or transfer matrices [5,6]. There is a nonzero ground state entropy of 0.2916 per site [1]. The correlation functions are critical (power-law decaying). This is easiest understood after mapping the dimer packings (configuration-by-configuration) to configurations of “heights” $z(\mathbf{r})$ living on dual lattice sites, $\mathbf{r} = (x, y)$, representing a rough interface in an 3-dimensional abstract space [7–12].

The explicit rule for constructing the heights is shown in Fig. 1: $z(\mathbf{r}) - z(\mathbf{r}') = -3$ if there is a dimer between \mathbf{r} and \mathbf{r}' , or $+1$ if there is no dimer, where the step from \mathbf{r} to \mathbf{r}' is taken in a counterclockwise sense about the even sites. Periodic boundary conditions are assumed for the dimers; we shall furthermore restrict configurations to those which have no net tilt, so that $z(\mathbf{r})$ also satisfies periodic boundary conditions.¹ (To relate $z(\mathbf{r}, t)$ at

different times, we specify that a dimer flip on a plaquette only changes $z(\mathbf{r})$ in the center of that plaquette.)

It is possible to turn any dimer covering (of zero mean tilt) into any other one by a succession of “dimer flips” each affecting two dimers on opposite edges of one plaquette (see Fig. 1(b)). Thus the model is endowed with a stochastic (Monte Carlo) dynamics in continuous time as follows: select plaquettes at random, at a rate N per unit time where $N \equiv L^2$ is the number of sites (i.e. on average visit each plaquette once per unit time). Flip the plaquette if it has two dimers as in Fig. 1(b), otherwise do nothing.

Let $\{p_\alpha(t)\}$ be the probability of being in microstate α at time t . The master equation states

$$\frac{dp_\alpha(t)}{dt} = \sum_{\langle \alpha \rightarrow \beta \rangle} (p_\beta - p_\alpha) \equiv - \sum_\beta \mathcal{W}_{\alpha\beta} p_\beta \quad (1)$$

where $\langle \alpha \rightarrow \beta \rangle$ means summing over configurations β which differ from α by one dimer flip; thus

$$\mathcal{W}_{\alpha\beta} = F_\alpha \delta_{\alpha\beta} - \mathcal{A}_{\alpha\beta} \quad (2)$$

where \mathcal{A} is the adjacency matrix (elements unity if α and β are related by a flip, and zero otherwise), and $F_\alpha \equiv \sum_\beta \mathcal{A}_{\alpha\beta}$ is the number of “flippable” plaquettes in configuration α . These matrices are $M_0 \times M_0$, where M_0 is the number of microstates. It is well known that the matrix \mathcal{W} has nonnegative eigenvalues (via the Perron-Frobenius theorem, since \mathcal{W} is a stochastic matrix). The eigenvector of zero eigenvalue is $p_\alpha = 1/M_0$, the weight of the (equilibrium) steady state (which is unique, since dimer flips connect all microstates). Furthermore, any time correlation function in the system can be resolved into a sum over eigenvalues λ of \mathcal{W} , in the form

$$\sum_\lambda c_\lambda e^{-\lambda t} \quad (3)$$

Then it is normal to define the system’s equilibration time

$$\tau(L) = \lambda'_{\min}^{-1}, \quad (4)$$

where λ'_{\min} is the smallest nonzero relaxation rate.

The main question addressed in this paper is, what is the equilibration time $\tau(L)$ of the system, defined as

¹In general, periodic boundary conditions for dimers only imply $z(L, y) - z(0, y) = \rho_x$ and $z(x, L) - z(x, 0) = \rho_y L$, where the “winding numbers” ρ_x and ρ_y are multiples of 4,

and thus the mean tilt is $(\rho_x/L, \rho_y/L)$.

the inverse of the second smallest eigenvalue of \mathcal{W} , as a function of its diameter L ? In particular, what is the dynamic exponent z [15] in $\tau(L) \sim L^z$? It has been proven [13] that (with our definition of time scale) $\tau(L) < O(N^3)$, which implies $z < 6$.

In this paper, I first argue that $z = 2$, on the basis of a standard Langevin equation which makes essential use of the height representation (Secs. II); a byproduct is an approximate description of *all* the slow eigenmodes (Sec. III). Then I outline a proof (in Sec. IV) that $\tau(L) > O(L^2)$ (and hence $z \geq 2$.) The fundamental concepts of this proof are (i) the use of Fourier analysis to partially diagonalize the evolution matrix \mathcal{W} , and (ii) taking advantage of our knowledge of the Fourier spectrum of height fluctuations from the exact solution of the model. In the conclusion, I mention other spin models (including the quantum dimer model) to which these results should be relevant.

II. CONTINUUM THEORY OF DYNAMICS

This section develops the continuum, (“coarse-grained”) version of the dynamics. In this form the model has an easily visualized physical meaning and (being linear) is solvable by standard and almost trivial techniques. In general, the slowest modes are associated with relaxation of the “order parameter” [14,15]; in the dimer covering model, the height variable plays the role of a (hidden) order parameter, so the dynamics are phrased in terms of it.

A. Continuum equations

First I review the coarse-grained picture of the height dynamics. The static free energy functional has the form

$$F = \int d^2\mathbf{r} \frac{K}{2} |\nabla h(\mathbf{r})|^2 \quad (5)$$

Here $h(\mathbf{r})$ represents a smoothed version of $z(\mathbf{r})$ and K is the stiffness constant controlling the fluctuations of the “interface”. The customary dynamics for such a field theory (see, e.g., [14]) is formulated as a Langevin equation,

$$\frac{dh(\mathbf{r})}{dt} = -\Gamma \frac{\delta F(\{h(\cdot)\})}{\delta h(\mathbf{r})} + \zeta(\mathbf{r}, t) \quad (6)$$

Here Γ is the kinetic (damping) constant measuring the linear-response to the force $\delta F/\delta h(\mathbf{r})$, and $\zeta(\mathbf{r}, t)$ is a random source of Gaussian noise, uncorrelated in space or in time. In order that Eq. (6) have for its steady state $\exp(-F)$ with F given by Eq. (5), the usual condition

$$\langle \zeta(\mathbf{r}, t) \zeta(\mathbf{r}', t') \rangle = 2\Gamma \delta(\mathbf{r} - \mathbf{r}') \delta(t - t') \quad (7)$$

must be satisfied.

To make plausible the assumption of uncorrelated noise, one must consider the action of the microscopic dynamics on the microscopic heights $z(\mathbf{r})$. An elementary dimer flip changes $z(\mathbf{r})$ on just one plaquette by $\pm\Delta z \equiv \pm 4$, and the next dimer flip occurs at another random place. Thus the net height is not conserved, the change is local, and uncorrelated in time, which are modeled by the identical properties of the Langevin noise in (7).

B. Fourier modes $\tilde{h}_\mathbf{q}$

We can Fourier transform the above equations, since periodic boundary conditions maintain translational symmetry. My short-distance cutoff prescription for this continuum field theory shall be that the fields’ Fourier transforms have support only in the Brillouin zone $(-\pi, \pi)^2$; in other words, the only allowed \mathbf{q} values are those which are defined for the microscopic lattice model (see Sec. IV). Then (6) becomes

$$\frac{d\tilde{h}_\mathbf{q}}{dt} = -\Gamma K |\mathbf{q}|^2 \tilde{h}_\mathbf{q} + \tilde{\zeta}_\mathbf{q}(t) \quad (8)$$

with Gaussian noise

$$\langle \tilde{\zeta}_\mathbf{q}(t)^* \tilde{\zeta}'_\mathbf{q}(t') \rangle = 2\Gamma \delta_{\mathbf{q},\mathbf{q}'} \delta(t - t'). \quad (9)$$

(Note that $\delta_{\mathbf{q},\mathbf{q}'}$ is the discrete δ -function, appropriate to the discrete lattice of wavevectors corresponding to periodic boundary conditions.)

Thus the different Fourier components are decoupled in (8). For each of them, (8) is the trivially soluble one-dimensional Langevin equation; its correlation function is

$$\langle \tilde{h}_\mathbf{q}(0) \tilde{h}_{-\mathbf{q}}(t) \rangle = \frac{1}{K |\mathbf{q}|^2} e^{-\lambda_h(\mathbf{q})t}, \quad (10)$$

where the relaxation rate is

$$\lambda_h(\mathbf{q}) = \Gamma K |\mathbf{q}|^2 \quad (11)$$

Strictly speaking, the dynamic exponent is defined by the relation between relaxation rates and wavevectors [15], thus (11) implies $z = 2$. As a corollary to (11), the smallest relaxation rate of a Fourier mode corresponds to the smallest nonzero wavevector $\mathbf{q}_{min} = (2\pi/L, 0)$ i.e.

$$\lambda_h(\mathbf{q}_{min}) = (4\pi^2 \Gamma K) L^{-2} \quad (12)$$

In the context of models of real (rough) interfaces of crystals, Eq. (6) is known as the Edwards-Wilkinson process [16]. There is a large literature on more elaborate equations of this form (usually with nonlinear terms) [17].

Scaling with dynamic exponent $z = 2$ has indeed been observed in simulations of the square lattice dimer covering [20] (using non-Fourier analysis). Rather than periodic boundary conditions, that work used “Aztec diamond” boundary conditions [3] such that $h(\mathbf{r})$ is fixed

(and spatially nonconstant) along the edges; the continuum equations would still predict $\tau(L) \sim L^2$ in that geometry.

Random tilings, with vertices not constrained to lie on a periodic lattice, are studied as models of quasicrystals [18]. These too can be mapped to effective interfaces $z(\mathbf{r})$. (A complication, unimportant for the present discussion, is that the height function $z(\mathbf{r})$ or $h(\mathbf{r})$ has two or more components in the quasicrystal cases.) In one case of a quasicrystal random tiling (in three spatial dimensions), (11) was confirmed by simulation [19]. After $z(\mathbf{r}, t)$ was constructed, the data were numerically Fourier transformed to give $\tilde{z}_{\mathbf{q}}(t)$ at selected (small) wavevectors \mathbf{q} ; for \mathbf{q} small, that is essentially $\tilde{h}_{\mathbf{q}}(t)$. Then the time correlations $\langle \tilde{z}_{\mathbf{q}}(0) \tilde{z}_{\mathbf{q}}(t) \rangle$ were fitted to the form (10) and a plot of $\lambda_h(\mathbf{q})$ versus \mathbf{q} revealed the behavior (11). Very recently, [12] has confirmed $z = 2$ in the same fashion for an Ising model with height representation.

C. Random walk of mean height

There is another sort of slow dynamics in the system, associated with symmetry under shifts, not in real space but in “height space” (the target space of $z(\mathbf{r})$ and $h(\mathbf{r})$). Consider the average height

$$\bar{h}(t) \equiv N^{-1} \int d^2 \mathbf{r} h(\mathbf{r}, t) \quad (13)$$

i.e. $N^{-1/2} \tilde{h}_0(t)$ (the factor $N^{1/2}$ comes from our normalization convention for Fourier transforms.) The Langevin equation (6) with $|\mathbf{q}| = 0$ tells us $\tilde{h}_0(t)$ simply executes a Gaussian random walk. So

$$\langle |\bar{h}(t) - \bar{h}(t')|^2 \rangle = D(N)t \quad (14)$$

with a diffusion constant

$$D(N) = 2\Gamma N^{-1}. \quad (15)$$

It is interesting that although the continuum theory cannot provide the numerical value of the coefficient Γ , it does predict an exact ratio (in the limit $N = L^2 \rightarrow \infty$) between the relaxation rate of the modulation $h(\mathbf{q}_{min}, t)$, and the diffusion rate of the wandering of $\bar{h}(t)$.

III. FOKKER-PLANCK MODES

If the picture introduced in Sec. II is a valid coarse-graining of the microscopic model, then *all* the low-lying eigenvalues of \mathcal{W} should be understood in terms of (6). So far we have only identified N Fourier modes in Subsec. II B, and the random walk of $\bar{h}(t)$ in Subsec. II C has not been related to *any* eigenmode. On the other hand, there are M linear modes of (1). (Recall $\ln M \sim N$.)

As we shall see, many of these have rates comparable to those of the Fourier modes in Sec. II. (Though even more of them are localized relaxations with rates of order unity, which cannot be captured properly in a coarse-grained model.)

These modes are of interest because (i) they are responsible for the deviations of the correlation functions from being pure exponentials; (ii) the analytic form of the modes, derived below, might inspire improvements on the variational eigenfunctions used in Sec. IV, and (iii) these modes correspond to excited states in the quantum dimer model at its critical point (see Subsec. V C).

A. Fourier modes

In fact, the precise analog of (1) is not (6), but the familiar Fokker-Planck equation for the evolution of the probability density $P(\{\tilde{h}_{\mathbf{q}}(t)\})$:

$$\frac{d}{dt} P(\{\tilde{h}_{\mathbf{q}}(t)\}) = \mathcal{W}_h \{P(\{\tilde{h}_{\mathbf{q}}(t)\})\} \quad (16)$$

$$\equiv \Gamma \frac{d}{d\tilde{h}_{\mathbf{q}}} \left[\frac{d}{d\tilde{h}_{-\mathbf{q}}} - K|\mathbf{q}|^2 \tilde{h}_{\mathbf{q}} \right] P(\{\tilde{h}_{\mathbf{q}}(t)\}) \quad (17)$$

Since $h_{\mathbf{q}}^* \equiv h_{-\mathbf{q}}$, we must consider $h_{\mathbf{q}}$ and $h_{-\mathbf{q}}$ together. ² Eq. (17) has one zero eigenvalue, corresponding to the Gaussian

$$\Psi_0 \equiv \exp\left(-\sum_{\mathbf{q} \neq 0} \frac{1}{2} K |\mathbf{q}|^2 \tilde{h}_{\mathbf{q}} \tilde{h}_{-\mathbf{q}}\right) \quad (18)$$

To construct all the other eigenfunctions, we define a “raising operator”

$$\mathcal{C}_{\mathbf{q}} \equiv \frac{d}{d\tilde{h}_{-\mathbf{q}}} + K|\mathbf{q}|^2 \tilde{h}_{\mathbf{q}} \quad (19)$$

It can be checked that

$$\mathcal{W}_h \mathcal{C}_{\mathbf{q}} - \mathcal{C}_{\mathbf{q}} \mathcal{L}_h = \lambda_h(\mathbf{q}) \mathcal{C}_{\mathbf{q}} \quad (20)$$

and further that $\{\mathcal{C}_{\mathbf{q}}\}$ commutes with $\{\mathcal{C}_{\mathbf{q}'}\}$ for all \mathbf{q}' , even $-\mathbf{q}$. Then we can write

$$\Psi(\{\tilde{h}_{\mathbf{q}}\}; \{n(\mathbf{q})\}) = \prod_{\mathbf{q} \neq 0} (\mathcal{C}_{\mathbf{q}})^{n(\mathbf{q})} \Psi_0(\{\tilde{h}_{\mathbf{q}}\}) \quad (21)$$

where $\{n(\mathbf{q})\}$ are nonnegative integers. The corresponding eigenvalue is

² The most proper way to solve (17) is in terms of $\text{Re } h(\mathbf{q})$ and $\text{Im } h(\mathbf{q})$. Now, given h is a complex variable, with $d/dh = d/d(\text{Re } h) - id/d(\text{Im } h)$, it follows that $dh^*/dh = 0$, which justifies the manipulations in (17) – (21).

$$\lambda_{tot}(\{n(\mathbf{q})\}) = \sum_{\mathbf{q} \neq 0} n(\mathbf{q}) \lambda_h(\mathbf{q}) \quad (22)$$

The net wavevector is

$$\mathbf{q}_{tot} = \sum_{\mathbf{q} \neq 0} n(\mathbf{q}) \mathbf{q}. \quad (23)$$

Note the degeneracies resulting from the fact that $\lambda(\mathbf{q}) = \lambda(-\mathbf{q})$.

This mathematical structure is virtually identical to that of a collection of quantized harmonic oscillators, with energy corresponding to (22) and $n(\mathbf{q})$ corresponding to the occupation number of oscillator \mathbf{q} . The unique $\lambda_{tot} = 0$ mode of the system corresponds to $n(\mathbf{q}) \equiv 0$ for all \mathbf{q} , as in the oscillator ground state. The modes of Subsec. II B are “elementary excitations” in which one $n(\mathbf{q}) = 1$ for one wavevector and zero for all the others. The slowest such mode is still (12).

Since there is no upper bound on $n(\mathbf{q})$, we have now obtained (infinitely) *more* modes of the continuum model than of the discrete model. Presumably, when $n(\mathbf{q})$ is so large that λ_{tot} is of order unity, the corresponding modes become ill-defined. Adopting the approximate upper cutoff $n_{max}(\mathbf{q}) \cong \text{const}/|\mathbf{q}|^2$, the total number of well-defined modes M_h indeed satisfies $\ln(M_h) \sim N \sim \ln(M_0)$.

B. Random walk of $\bar{h}(t)$ ($\mathbf{q} = 0$ modes)

The above description (see (22) omitted the $\mathbf{q} = 0$ mode. Here, eigenfunctions of the Fokker-Planck equation for \bar{h} are

$$\psi_Q(\bar{h}) = \exp(iQ\bar{h}) \quad (24)$$

for any Q , which would give a continuum of eigenvalues

$$\lambda(0, Q) = \frac{1}{2}D(N)Q^2 \quad (25)$$

with $D(N)$ given by (15). In fact, however, a global shift $z(\mathbf{r}) \rightarrow z(\mathbf{r}) + 4$ of a microstate corresponds to the same microstate. Thus, the only modes which can correspond to modes in the microscopic model are those periodic under $h(\mathbf{r}) \rightarrow h(\mathbf{r}) + 4$; i.e.

$$Q = n(0)\frac{\pi}{2} \quad (26)$$

for any integer $n(0)$. Thus, the *complete* eigenmodes are products of (22) with (24) for any integer $n(0)$ in (26); the corresponding eigenvalue is $\lambda_{tot} + (\pi^2\Gamma/4N)n(0)^2$.

The eigenvalue given by $n(0) = \pm 1$,

$$\lambda(0, \pi/2) = \frac{\pi^2}{4}\Gamma N^{-1} \quad (27)$$

is in fact the smallest nonzero eigenvalue,³ smaller than (12) by a factor $(16K)^{-1}$ (assuming $N = L^2$, and using the exact value $K = \pi/16$, see Appendix.)

IV. MICROSCOPIC THEORY

Now we return to the exact microscopic dynamics, as introduced in Sec. I. The microstates are viewed as nodes of a graph in an abstract space, with each possible dimer-flip (and its inverse) forming an edge of the graph: the dynamics described by (1) is a random walk on this graph. As noted already, the graph of microstates with tilt zero has only one connected component. The matrix \mathcal{W} is not only stochastic but symmetric.

A. Variational bound

The key idea in this section is the use of a variational guess for the eigenfunction. This is mathematically equivalent to the variational bound on the eigenenergy in the quantum dimer model (see Subsec. V C and [21]).

For any vector $\{\phi_\alpha\}$, the smallest eigenvalue λ_{min} satisfies

$$\lambda_{min} \leq \lambda_\phi \equiv \frac{(\phi^* \mathcal{W} \phi)}{(\phi^* \phi)} \quad (28)$$

Here ϕ^* means the hermitian conjugate. From (2), the numerator is

$$(\phi^* \mathcal{W} \phi) = \sum_{\langle \alpha \beta \rangle} |\phi_\alpha - \phi_\beta|^2 \quad (29)$$

where $\langle \alpha \beta \rangle$ means every pair of microstates, connected by a spin flip, is counted once.

In the two cases considered in this paper (following subsections), $|\phi_\alpha - \phi_\beta| \equiv |\Delta\phi|$ turns out to be the same for every flip move. Then the sum (29) reduces to $\frac{1}{2}|\Delta\phi|^2 \sum_\alpha F_\alpha$ (the $1/2$ cancels the double-counting of each graph edge), and finally to $\frac{1}{2}fN|\Delta\phi|^2$. Here f is the probability that a given plaquette is “flippable”, i.e. fN is the average “coordination number” of the microstate graph. The exact value [22] is

$$f = 1/8. \quad (30)$$

Meanwhile, the denominator in (28) is just $M_0(\langle \phi \rangle^2)$. Thus finally the upper bound is

³ Of course, (27) would not be smallest in the case of $h(\mathbf{r})$ fixed along the boundaries, as in [3] and [13], since that forbids \bar{h} -wandering modes.

$$\lambda_\phi = \frac{1}{2} f N \frac{|\Delta\phi|^2}{\langle |\phi|^2 \rangle} \quad (31)$$

When applied to the entire set of eigenvalues of \mathcal{W} , eq. (31) is not very interesting, since we already know that $\lambda_{min} = 0$ (the eigenvalue of the steady state). However, the variational argument (and every equation in this subsection) is also valid when restricted to a *subspace* orthogonal to that of the ground state. Then, the bound (31) can be useful since the λ_{min} of such a subspace is usually positive.⁴ Indeed, the overall smallest nonzero eigenvalue – the goal of this paper (see (4)) – is expected to be the λ_{min} of one of these subspaces.

The above variational argument was first presented [23] with a physical interpretation in terms of the normalized dynamic correlation function

$$C_\phi(t) \equiv \frac{\langle \phi(0)^* \phi(t) \rangle}{\langle |\phi|^2 \rangle} \quad (32)$$

Then $C_\phi(t) = 1 - \frac{1}{2} \langle |\phi(0) - \phi(t)|^2 \rangle / \langle |\phi|^2 \rangle$; but at short times, $\langle |\phi(0) - \phi(t)|^2 \rangle \cong \langle |\Delta\phi|^2 \rangle f N t$, since there are on average $f N$ independent places where a flip could occur. Thus the upper bound on λ_{min} can be rewritten as the *initial* decay rate of the correlation function, [23]

$$\lambda_\phi = -\frac{dC_\phi(t)}{dt} \Big|_{t=0} \quad (33)$$

Ref. [23] (and similarly [24]) applied (33) to bounding the dynamic critical exponent by a function of the static exponents (for a system with nontrivial exponents).

In some circumstances, λ_ϕ could be a good estimate of λ_{min} . It would be exact if subsequent steps in ϕ were uncorrelated. (We assume our variational ϕ_α always has nonzero projection onto the slowest mode.) Then $\phi(t)$ performs a random walk, and $C_\phi(t) = \exp(-\lambda_\phi t)$, a pure exponential decay. In light of (3), in which coefficients allowed by symmetry are expected to be generically positive, we would obtain $\lambda_{min} = \lambda_\phi$.

However, dynamics actually adopted (in eq. (1)) is such that the steps are manifestly anticorrelated in time. For, if a plaquette flips, it will undergo the reverse flip the next time it is visited, unless its configuration has been shuffled in the meantime by flips of the adjoining plaquettes. So we expect $\lambda_{min} < \lambda_\phi$ (strictly).

B. Fourier modes

First we review the use of basis states with definite \mathbf{q} vectors. Consider the action of a translation of \mathbf{r} ;

this induces a permutation of microstates which manifestly commutes with \mathcal{W} . Thus all eigenvectors must have a definite wavevector \mathbf{q} (or can be chosen thus); that is, a translation by \mathbf{r} simply induces a multiplication by $\exp(i\mathbf{q} \cdot \mathbf{r})$ of the eigenvector. Furthermore \mathcal{W} must have zero matrix elements between vectors with different \mathbf{q} ; thus \mathcal{W} becomes block-diagonal in the new basis of states with definite \mathbf{q} .⁵ Hence (28) is valid for the smallest eigenvalue $\lambda_{min}(\mathbf{q})$ in each block of definite \mathbf{q} ; that is, if $\{\phi_\alpha\}$ has wavevector \mathbf{q} , then

$$\lambda_{min}(\mathbf{q}) \leq \frac{(\phi^* \mathcal{W} \phi)}{(\phi^* \phi)} \quad (34)$$

A suitable variational state-space vector (for $\mathbf{q} \neq 0$) is suggested by the “elementary excitation” eigenfunctions of Subsec. III A; they consisted of the steady-state eigenfunction Ψ_0 multiplied by \tilde{h}_q . The microscopic analog of the gaussian Ψ_0 is the equal-weighted eigenfunction of \mathcal{W} , hence we choose

$$\phi_\alpha^{(\mathbf{q})} \equiv \tilde{z}_\mathbf{q}(\alpha) \quad (35)$$

(Here $\tilde{z}_\mathbf{q}(\alpha)$ means take the configuration $z(\mathbf{r})$ corresponding to microstate α and Fourier transform it for wavevector \mathbf{q}). This approach – constructing a variational vector from the Fourier transform of a local operator – is essentially the “single-mode approximation” used for quantum many-body systems such as superfluid helium [25].

If α, β are related by one dimer flip on the plaquette at \mathbf{r}_f , the corresponding configurations of $z(\mathbf{r})$ differ only by $\pm \Delta z \equiv \pm 4$ at \mathbf{r}_f . Consequently $|\Delta\phi|^2 = |\Delta z|^2/N$. On the other hand, the denominator of (28) is exactly

$$\sum_\alpha |\tilde{z}_\mathbf{q}(\alpha)|^2 = M_0 \langle |\tilde{z}(\mathbf{q})|^2 \rangle \quad (36)$$

(recall each microstate is weighted equally). Thus the variational bound has the form

$$\lambda_{min}(\mathbf{q}) \leq 8f / \langle |\tilde{z}(\mathbf{q})|^2 \rangle \quad (37)$$

Finally, we know $\langle |\tilde{z}(\mathbf{q})|^2 \rangle \cong 1/K|\mathbf{q}|^2$ at small \mathbf{q} , as derived in the Appendix, Eq. (A10). This gives the result (for small \mathbf{q})

$$\lambda_{min}(\mathbf{q}) \leq 8fK|\mathbf{q}|^2. \quad (38)$$

If we assume (11), then (38) gives a bound on the kinetic coefficient:

$$\Gamma \leq \frac{1}{2}(\Delta z)^2 f \equiv 8f \quad (39)$$

⁴In subsequent subsections, labels will be attached to λ_{min} to indicate which subspace they belong with, but the labels have been omitted in the general argument here.

⁵I have not bothered to take advantage of the additional lattice symmetries (rotations by $\pi/2$ and reflections), which would permit a bit more block-diagonalization.

C. Random walk of $\bar{z}(t)$

The variational trick also works for the random walk behavior of (15). Obviously the microscopic analog of (13) is

$$\bar{z}(t) \equiv N^{-1} \sum_{\mathbf{r}} z(\mathbf{r}, t), \quad (40)$$

Then the $\mathbf{q} = 0$ modes can be further block-diagonalized into modes with particular wavevectors Q in height space, as defined in Subsec. III B, hence the variational bound is valid within each such block (to be labeled “ $(0; Q)$ ”).

In analogy to (24), we use the variational vector

$$\phi_{\alpha}^{(0; Q)} \equiv e^{iQ\bar{z}(\alpha)} \quad (41)$$

In this case, $|\Delta\phi| = |\sin(Q\Delta z/2N)|$ for any state α , with $\Delta z = \pm 4$ the same as before, and obviously $|\phi_{\alpha}| = 1$ in any state. So from (31) we obtain the bound $\lambda_{\min}(0; Q) \leq \frac{1}{2}fN \sin^2(4Q/N)$, or

$$\lambda_{\min}(0; Q) \leq 8f(\pi/2)^2/N \quad (42)$$

for large N .

Just like the results (11) and (25) for the two respective kinds of mode in the continuum model, the best variational upper bounds for slow relaxation rates in the microscopic model correspond respectively to $|\mathbf{q}| = |\mathbf{q}_{\min}| = 2\pi/L$ in (38) or to $Q = \pi/2$ in (42). Either kind of bound implies a lower bound on the relaxation time τ which is $O(L^2)$. The better bound comes from (39), and after substituting the value of f (30) gives

$$\tau \geq (2/\pi)^2 N. \quad (43)$$

It is interesting to note that (42), when compared to (15) and (25), gives the same bound on Γ as Eq. (39) derived from Fourier modes. This might be taken as an approximation for Γ , which amounts (as already noted) to neglecting the anticorrelation of flips. Such an approximation for Γ was made in a random tiling quasicrystal model. (See Sec. IV A and footnote 36 of Ref. [19]). It turned out [19] to overestimate the true Γ (estimated from the simulation) by about 50%.

V. DISCUSSION

A. Summary

The results in Secs. II and IV exemplify the fruitfulness of Fourier analysis in models with translational symmetry; indeed two types of Fourier transform were used, one (Subsecs. II B, III A, and IV B) conditioned on translations in physical space, and the other (Subsecs. II C, III B, and IV C) on translations in “height space”. For

each type, two arguments have been given, one based on a coarse-grained field theory (Secs. II and III) and the other based on exact bounds (Sec. IV), which indicate the the longest relaxation time scales with system size as L^2 .

The only rigorous consequence of the present argument is a *lower* bound (43) on the longest relaxation time. For computational purposes one prefers, of course, an *upper* bound on the time needed to equilibrate the system. Towards this end, the present calculation merely suggests the possible usefulness of Fourier analysis in such a demonstration, and warns that the slowest mode is not a Fourier modulation at all but the “ \bar{z} diffusion” (see Subsec. III B).

B. Computational physics

This study is relevant to the dynamics of other spin models. In particular, its results apply directly to the critical dynamics of the fully-frustrated Ising model on the square lattice since that model (at its critical temperature, $T_c = 0$) maps to the dimer covering [4]. The derivations could be trivially adapted to the dimer covering of the honeycomb lattice and hence to the critical ($T_c = 0$) dynamics of the triangular Ising antiferromagnet (equivalent to the dimer covering [7]). The behavior argued here can be expected in other spin models which have height representation and single-spin update rules, e.g. the $T = 0$ three-state Potts antiferromagnet on the square lattice (equivalent to the 6-vertex model [26] and hence the BCSOS model). In those cases, however, no exact results or rigorous bounds for the static fluctuations are available to replace the Appendix.

Understanding the local dynamics addressed here is also a prerequisite to addressing the dynamics of height models endowed with loop-update or cluster-update rules, including fully-frustrated Ising models [27], the three-state Potts antiferromagnet on the square lattice [28], the BCSOS model [29], and coloring models [30].⁶ More speculatively, it would be interesting to check whether there is any connection between the Swendsen-Wang [34] algorithm and the height representation in the case of the ferromagnetic 4-state Potts model, the partition function of which can be mapped to that of a height model [31].

Somewhat analogous to the loop-update rules are the “zipper moves” [18,32] of certain random tiling quasicrystal models, such as the (two-dimensional) square-triangle

⁶It turns out that all the algorithms cited have a simple action on the height variables, thus the existence of a height map may be a prerequisite to the possibility of accelerating such models.

random tiling. In that case, the correlation time was measured to be of $O(1)$ update move per site [32]; however each update move involved $O(L^2)$ sites, so the scaling of the net correlation time was $O(N^2)$ just as for the local dimer flip dynamics treated in the present paper.

The height field is the hidden order parameter in the present model (or of height models in general) and hence is the proper way to approach the coarse-grained, long time dynamics. Note that experience has shown that the *static* exponents are extracted much more efficiently from $\langle |h(\mathbf{q})|^2 \rangle$ than from spin-spin correlations (using the same simulations) [30,11,33]. Therefore, I suggest numerical studies of the dynamics ought to extract estimates of the correlation times directly from the height fields rather than from spin-spin correlations.

C. Quantum dimer model

In the quantum dimer model, the basis states are taken to be the dimer coverings, and the Hamiltonian is taken to have matrix elements

$$\mathcal{H}_{\alpha\beta} = -t\mathcal{A}_{\alpha\beta} + V\delta_{\alpha\beta}F_\alpha. \quad (44)$$

The first term describes dimer flips – like a particle quantum “hopping” with amplitude t on the microstate graph; the second term is a “potential energy” which penalizes each flippable plaquette.

When $V/t = 1$, obviously

$$\mathcal{H}_{\alpha\beta} \propto \mathcal{W}_{\alpha\beta} \quad (45)$$

Ref. [35] noted that (45) implies the ground state wavefunction of (44) is a superposition of all the dimer packings with equal amplitudes. In other words, that (quantum) wavefunction is proportional to the steady-state probabilities of the (classical) dynamics (1). I note that (45) further implies a one-to-one correspondence of *all* the eigenstates of (44) to normal modes of the master equation. In particular, the low-energy excited states of the quantum system (which are found from exact-diagonalization studies up to 8×8 lattices [36]) should have energies $\omega(\mathbf{q}) \cong \Gamma K |\mathbf{q}|^2$ [21].

ACKNOWLEDGMENTS

I am grateful to D. Randall, and P. W. Leung for stimulating discussions, and to C. Zeng for helpful comments on the manuscript. I thank the Institute for Advanced Study for hospitality. This work was supported by NSF grant DMR-9214943.

APPENDIX A: STATIC FLUCTUATIONS

This appendix reviews what is known exactly about the equal-time fluctuations of Fourier components of $z(\mathbf{r})$. This result will be an essential lemma for the proof about $\lambda(\mathbf{q})$ outlined in Sec. IV.

Evidently, in the continuum picture, the equal-time expectations are given by

$$\langle \tilde{h}_{\mathbf{q}}^* \tilde{h}_{\mathbf{q}'} \rangle = \delta_{\mathbf{q},\mathbf{q}'} \frac{1}{K|q|^2} \quad (A1)$$

(Recall that $\tilde{h}_{\mathbf{q}}^* \equiv \tilde{h}_{-\mathbf{q}}$.) This scaling is equivalent to

$$\langle |h(\mathbf{r}) - h(\mathbf{r}')|^2 \rangle = O(1) + \frac{1}{2\pi K} \ln |\mathbf{r} - \mathbf{r}'| \quad (A2)$$

in direct space.

In the study of “height models” [11,30,33,12] and random-tiling quasicrystals [18], it is the fundamental hypothesis that $\tilde{z}(\mathbf{q})$ has a behavior like (A1) at small \mathbf{q} . The behavior (A1) has been proven rigorously for a very limited set of discrete models [37], and not even for the well-known BCSOS model of rough interfaces [38]. Even though the latter model is “exactly soluble” [39] via the Bethe ansatz, such correlation functions are not known exactly (correlation functions are notoriously difficult to extract from the Bethe ansatz method [42]).

However, the dimer covering model (with 2D Ising models) belongs to the “free-fermion” class of exactly soluble models [1,2], and using the Pfaffian approach the dimer-dimer correlation functions can (in principle) be written out exactly [22]. Later on McCoy evaluated the large-distance asymptotic behavior of the correlation function, for any orientation of the vector between the two dimers [40].

Say that $n_x(\mathbf{r}) = 1$ when there is a dimer connecting \mathbf{r} to $\mathbf{r} + [1, 0]$ and zero otherwise; $\delta n_x(\mathbf{r}) \equiv n_x(\mathbf{r}) - \langle n_x(\mathbf{r}) \rangle \equiv n_x(\mathbf{r}) - \frac{1}{4}$, similarly for $n_y(\mathbf{r})$.

It was computed [22] that, in the equal-weighted ensemble of dimer coverings,

$$C_{xx}(\mathbf{R}) \equiv \langle \delta n_x(\mathbf{r}) \delta n_x(\mathbf{r}') \rangle = -g(X, Y)^2 + g(X+1, Y)g(X-1, Y) \quad (A3)$$

Here $\mathbf{R} \equiv (X, Y) \equiv \mathbf{r}' - \mathbf{r}$, and $g(X, Y)$ is a Green’s function arising from the Pfaffians [22]. At large \mathbf{R} ,

$$g(X, Y) \cong \begin{cases} -\frac{1}{\pi R^2}, & X \text{ odd, } Y \text{ even;} \\ \frac{i}{\pi R^2}, & X \text{ even, } Y \text{ odd;} \\ 0 & \text{otherwise.} \end{cases} \quad (A4)$$

Hence, collecting the four cases (X and Y even or odd),

$$C_{xx}(X, Y) \cong \frac{1}{2\pi^2} [(-1)^{X+Y} \frac{Y^2 - X^2}{R^4} + (-1)^X \frac{1}{R^2}] \quad (A5)$$

Dimer correlations imply correlations in height gradients since the definition of $z(\mathbf{r})$ (Sec. I) is equivalent to

$$z(\mathbf{r} + [\frac{1}{2}, \frac{1}{2}]) - z(\mathbf{r} + [-\frac{1}{2}, \frac{1}{2}]) = (-1)^{x+y} 4\delta n_y(\mathbf{r}) \quad (\text{A6a})$$

$$z(\mathbf{r} + [\frac{1}{2}, \frac{1}{2}]) - z(\mathbf{r} + [\frac{1}{2}, -\frac{1}{2}]) = (-1)^{x+y+1} 4\delta n_x(\mathbf{r}) \quad (\text{A6b})$$

Combining (A5) and (A6b), with

$$z(\mathbf{r} + [\frac{1}{2}, \frac{1}{2}]) - z(\mathbf{r} + [\frac{1}{2}, -\frac{1}{2}]) \rightarrow \nabla_y z(\mathbf{r}) \quad (\text{A7})$$

gives

$$\langle \nabla_y z(\mathbf{r}) \nabla_{y'} z(\mathbf{r}') \rangle \cong \frac{4^2}{2\pi^2} \left[\frac{Y^2 - X^2}{R^4} + (-1)^Y \frac{1}{R^2} \right] \quad (\text{A8a})$$

The term in (A8a) multiplied by $(-1)^Y$ will be neglected since it averages to zero. Similarly, using the analogous formulas for $\langle \delta n_x \delta n_y \rangle$,

$$\langle \nabla_x z(\mathbf{r}) \nabla_{y'} z(\mathbf{r}') \rangle \cong -\frac{4^2}{2\pi^2} \frac{2XY}{R^4} \quad (\text{A8b})$$

and

$$\langle \nabla_x z(\mathbf{r}) \nabla_{x'} z(\mathbf{r}') \rangle \cong -\frac{4^2}{2\pi^2} \left[\frac{X^2 - Y^2}{R^4} + (-1)^X \frac{1}{R^2} \right] \quad (\text{A8c})$$

The non-oscillating correlations in Eqs. (A8) have the form of dipole-dipole interactions, as if $\nabla z(\mathbf{r})$ is a polarization. [40] Integrating these equations with respect to \mathbf{R} ,

$$\langle |z(\mathbf{r}) - z(\mathbf{r}')|^2 \rangle \cong \text{const} + \frac{16}{\pi^2} \ln |\mathbf{r} - \mathbf{r}'| \quad (\text{A9})$$

and Fourier transforming yields the required result,

$$\langle |\tilde{z}(\mathbf{q})|^2 \rangle \cong \frac{16}{\pi |\mathbf{q}|^2}. \quad (\text{A10})$$

The behavior is indeed described by the continuum mode (A1), with $K = \pi/16$.

An exact result for arrow-arrow correlations was also obtained for a special case of the 6-vertex model [6], and applied to compute exactly the coefficient of the logarithmic asymptotic behavior of $\langle |z(\mathbf{r}) - z(\mathbf{r}')|^2 \rangle$ for the corresponding BCSOS model [41]. (The BCSOS model is just the height mapping of the 6-vertex model). Actually, the parameter values in that special case make it equivalent to a random dimer covering. To convert the $h(\mathbf{r})$ of the dimer model to the height $h_{BCSOS}(\mathbf{r})$ of a BCSOS model (with lattice constant $\sqrt{2}$), put $h(\mathbf{r})/2 = h_{BCSOS}$ on the sublattice with even $h(\mathbf{r})$ and erase $h(\mathbf{r})$ on the sublattice where it is odd. (See also [43]; to relate this to other versions of the same mapping between models [44] reverse all the arrows pointing along vertical bonds).

- [1] M. E. Fisher, Phys. Rev. 124, 1664 (1961).
- [2] P. W. Kasteleyn, Physica 27, 1209 (1961).
- [3] H. Cohn, N. Elkies, and J. Propp, preprint “Local statistics for random domino tilings of the Aztec diamond”.
- [4] J. Villain, J. Phys. C10, 1717 (1977).
- [5] E. H. Lieb, J. Math. Phys. 8, 2339 (1967).
- [6] B. Sutherland, Phys. Lett. 26A, 532 (1968).
- [7] H. W. J. Blöte and H. J. Hilhorst, J. Phys. A 15, L631 (1982); B. Nienhuis, H. J. Hilhorst, and H. W. J. Blöte, J. Phys. A 17, 3559 (1984).
- [8] W. Zheng and S. Sachdev, Phys. Rev. B 40, 2704 (1989).
- [9] L. S. Levitov, Phys. Rev. Lett. 64, 92 (1990).
- [10] W. Thurston, Amer. Mathematical Monthly 97, 757 (1990).
- [11] R. Raghavan, C. L. Henley, and S. L. Arouh, “New two-color dimer models with critical ground states”, preprint cond-mat/9606220; to appear, J. Stat. Phys., 1997.
- [12] C. Zeng and C. L. Henley, unpublished.
- [13] M. Luby, D. Randall, and A. Sinclair, “Markov chain algorithms for planar lattice structures” (preprint).
- [14] P. M. Chaikin and T. C. Lubensky, *Principles of Condensed Matter Physics* (Cambridge University Press, 1995).
- [15] P. C. Hohenberg and B. I. Halperin, Rev. Mod. Phys. 49, 435 (1977).
- [16] S. F. Edwards and D. L. Wilkinson, P. Roy. Soc. Lond. A 381, 17 (1981).
- [17] A.-L. Barabasi and H. E. Stanley, *Fractal Concepts in Surface Growth* (Cambridge University Press, 1995).
- [18] C. L. Henley, in *Quasicrystals: The State of the Art*, ed. P. J. Steinhardt and D. P. DiVincenzo (World Scientific, 1991).
- [19] L. J. Shaw, V. Elser, and C. L. Henley, Phys. Rev. B43, 3423 (1991).
- [20] J. Propp, personal communication.
- [21] C. L. Henley, unpublished.
- [22] M. E. Fisher and J. Stephenson, Phys. Rev. 132, 1411 (1963).
- [23] B. I. Halperin, Phys. Rev. B 8, 4437 (1973).
- [24] X.-J. Li and A. D. Sokal, Phys. Rev. Lett. 63, 827 (1989).
- [25] R. P. Feynman, in *Progress in Low-Temperature Physics*, vol. 1, ed. C. Gorter (North-Holland, 1955).
- [26] E. H. Lieb and F. Y. Wu, in *Phase Transitions and Critical Phenomena v. I*, ed. C. Domb and M. S. Green. (Academic Press, 1972).
- [27] D. Kandel, R. Ben-av, and E. Domany, Phys. Rev. Lett. 65, 941 (1990); D. Kandel and E. Domany, Phys. Rev. B 43, 8539 (1991).
- [28] J.-S. Wang, R. H. Swendsen, and R. Kotecký, Phys. Rev. Lett. 63, 109 (1989); Phys. Rev. B 42, 2465 (1990).
- [29] H. G. Evertz, G. Lana, and M. Marcu, Phys. Rev. Lett. 70, 875 (1993).
- [30] J. Kondev and C. L. Henley, Phys. Rev. B 52, 6628 (1995).
- [31] B. Nienhuis, in *Phase Transitions and Critical Phenomena*, edited by C. Domb and J.L. Lebowitz (Academic, London, 1987), Vol. 11.
- [32] M. Oxborrow and C. L. Henley, Phys. Rev. B 48, 6966 (1993).
- [33] J. K. Burton and C. L. Henley, “Constrained antiferromagnetic Potts model with an interface representation”

preprint to be submitted to J. Phys. A.

[34] R. H. Swendsen and J-S. Wang, Phys. Rev. Lett. 58, 86 (1987).

[35] D. S. Rokhsar and S. A. Kivelson, Phys. Rev. Lett. 61, 2376 (1988).

[36] P. W. Leung, K. C. Chiu, and K. Runge, preprint (cond-mat/9605179) “Columnar dimer and plaquette resonating bond valence bond states of the quantum dimer model”.

[37] J. Fröhlich and T. Spencer, Phys. Rev. Lett. 46, 1006 (1981); Commun. Math. Phys. 81, 527 (1981).

[38] T. Spencer, private communication (1996).

[39] H. van Beijeren, Phys. Rev. Lett. 38, 993 (1977).

[40] R. W. Youngblood, J. D. Axe, and B. M. McCoy Phys. Rev. B 21, 5212 (1980). (see their Appendix A.)

[41] D. B. Abraham, in C. Domb and J. L. Lebowitz, *Phase Transitions and Critical Phenomena*, Vol. 10 (Academic Press, 1986); see his Sec. VII B.

[42] R. J. Baxter, *Exactly Solved Models in Statistical Mechanics* (Academic Press, 1982).

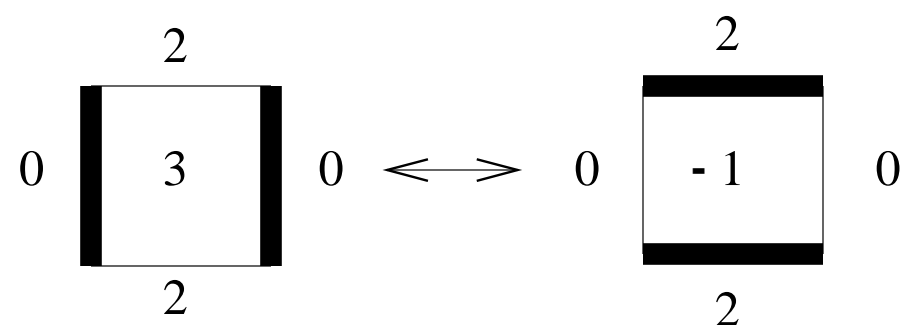
[43] R. J. Baxter, Ann. Phys. (N.Y.) 70, 193 (1972). (See Appendix A).

[44] B. Sutherland, unpublished.

FIG. 1. (a). Random dimer packing, showing heights $z(\mathbf{r})$ (those in flippable plaquettes are circled). (b). Elementary dimer flip, showing heights.

	2	1	(-2)	1	2	(5)
3	0	-1	0	3	4	
2	1	2	1	2	(1)	
3	(4)	3	(0)	3	4	
2	1	2	1	2	(5)	
3	0	-1	0	3	4	

(a)



(b)

